A statistical study of the propagation characteristics of whistler waves observed by Cluster

Oleksiy Agapitov, Vladimir Krasnoselskikh, Yuri V. Khotyaintsev, Guy Rolland

A statistical study of the propagation characteristics of whistler waves observed by Cluster

Oleksiy Agapitov,[1,2] Vladimir Krasnoselskikh,[1] Yuri V. Khotyaintsev,[3] and Guy Rolland[4]

Received 7 September 2011; revised 16 September 2011; accepted 16 September 2011; published 19 October 2011.

[1] VLF waves play a crucial role in the dynamics of radiation belts, and are responsible for the loss and the acceleration of energetic electrons. Modeling wave-particle interactions requires the best possible knowledge for how wave energy and wave-normal directions are distributed in L-shells and for the magnetic latitudes of different magnetic activity conditions. In this work, we performed a statistical study for VLF emissions using a whistler frequency range for nine years (2001–2009) of Cluster measurements. We utilized data from the STAFF-SA experiment, which spans the frequency range from 8.8 Hz to 3.56 kHz. We show that the wave energy distribution has two maxima around $L \sim 4.5 - 6$ and $L \sim 2$, and that wave-normals are directed approximately along the magnetic field in the vicinity of the geomagnetic equator. The distribution changes with magnetic latitude, and so that at latitudes of ~30°, wave-normals become nearly perpendicular to the magnetic field. The observed angular distribution is significantly different from Gaussian and the width of the distribution increases with latitude. Since the resonance condition for wave-particle interactions depends on the wave normal orientation, our results indicate that, due to the observed change in the wave-normal direction with latitude, the most efficient particle diffusion due to wave-particle interaction should occur in a limited region surrounding the geomagnetic equator. **Citation:** Agapitov, O., V. Krasnoselskikh, Y. V. Khotyaintsev, and G. Rolland (2011), A statistical study of the propagation characteristics of whistler waves observed by Cluster, *Geophys. Res. Lett.*, *38*, L20103, doi:10.1029/2011GL049597.

1. Introduction

[2] Discrete ELF/VLF (Extremely Low Frequency/Very Low Frequency) chorus emissions are one of the most intense electromagnetic plasma waves observed in radiation belts and in the outer terrestrial magnetosphere. Emissions are characterized by rising and falling tones, with frequencies ranging from a few hundred Hz to several kHz (see reviews by *Sazhin and Hayakawa* [1992] and *Omura et al.* [1991]). Since emissions play a crucial role in the local acceleration and loss of energetic electrons, they are important for the dynamics of the outer radiation belt. The resonant interaction of particles with VLF waves results in the diffusion of electrons in pitch angle and energy, and can lead to a violation of the first and second adiabatic invariants of particle motion (see review by *Shprits et al.* [2008]).

[3] The development of numerical models, such as the Radiation Belts Environment Model [*Fok et al.*, 2008], Salammbô model [*Bourdarie et al.*, 1996] or the model recently proposed by *Albert et al.* [2009], describing the dynamics of the outer radiation belt requires a knowledge of the diffusion coefficients related to the wave-particle interaction processes and of the distribution of wave power within the magnetosphere. In order to estimate pitch angle or energy diffusion coefficients, it is necessary to know the distribution of the wave intensity and the wave-normals for various plasma wave modes within and outside the outer radiation belt. Recently, several statistical models of wave distributions have been proposed by making use of wave measurement data obtained on board the Dynamic Explorer 1 (DE-1) [*Andre et al.*, 2002], CRRES [*Meredith et al.*, 2001, 2004], Cluster [*Pokhotelov et al.*, 2008], and THEMIS [*Cully et al.*, 2008] satellites. Most statistical models describe the dependencies of the averaged wave amplitude distributions on frequency, the L-shell, the magnetic latitude (MLat), and the magnetic local time (MLT). However, the properties of wave-vector distributions have not been statistically studied.

[4] The majority of models describing the formation and dynamics of the radiation belts treat the wave-particle interactions within VLF waves with a framework of quasi-linear approximation and should take into account the impact of the wave distribution in the magnetosphere on the L-shell. The process of particle diffusion is stated to be slow compared with the particle bounce time between reflection points along the magnetic field line. Thus, the diffusion coefficients were evaluated using averaging over fast time-scales, namely the gyro-period and the bounce time between reflection points. For the analysis, knowing the energy density of the waves in resonance with particles along a particular L-shell for different magnetic latitudes is required. A solution for this problem was proposed by Lyons and co-authors [*Lyons and Thorne*, 1973; *Lyons*, 1974a, 1974b] and was determined using the PADIE simulation code of *Glauert and Horne* [2005]. The wave distribution in these models was assumed to have a Gaussian dependence on the frequency and the angle between the wave-normal and the magnetic field. The results are quite sensitive to the characteristics of the assumed distribution [*Glauert and Horne*, 2005]. Therefore, previously obtained results that have been based on the mechanisms and the rates of relativistic electron acceleration and diffusion by chorus waves, have been based on time-averaged spectral densities, which, as we point out in this work, may not be representative of realistic conditions. Wave amplitudes also have a significant probability in the tail of the probability

[1] LPC2E, CNRS, Orleans, France.
[2] Astronomy and Space Physics Department, National Taras Shevchenko University of Kiev, Kiev, Ukraine.
[3] Swedish Institute of Space Physics, Uppsala, Sweden.
[4] CNES, Toulouse, France.

0094-8276/11/2011GL049597

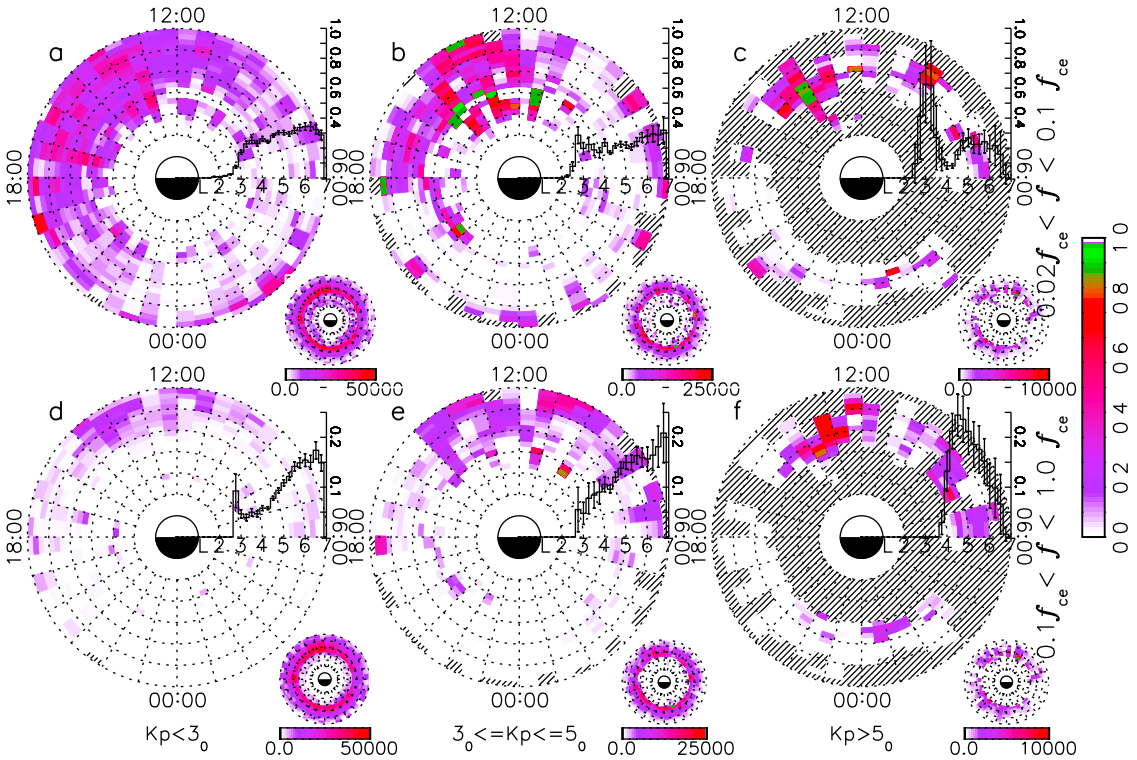

Figure 1. The occurrence rate for large amplitude whistler waves during periods of low ($K_p < 3$), intermediate ($3 \le K_p \le 5$), and high geomagnetic activity ($K_p > 5$). Whistler waves (top) in the hiss frequency range ($0.02f_{ce} < f < 0.1f_{ce}$) and (bottom) in the chorus frequency range ($0.1f_{ce} < f < 1.0f_{ce}$). The black line plots in each panel show the occurrence rate for large amplitude events as the ratio of the number of registered large amplitude waves to the total number of events in the L-shell bin. Data coverage for the CLUSTER STAFF-SA for each frequency and activity range is shown in the small inset.

distribution function [*Cully et al.*, 2008], which makes the use of averaged values potentially misleading. In order to improve the description of wave-particle interactions, one should take into account the inhomogeneity of the distribution of the wave electromagnetic field along the magnetic flux tube, and describe the effects of oblique wave propagation with respect to the background magnetic field. To achieve this objective, one first needs to determine the statistical distribution of wave-normals and wave amplitudes in the magnetosphere. The distribution of whistler wave-vector directions (the angle between the wave-vectors and the background magnetic field - θ) have mainly been studied in the vicinity of the equator [*Hayakawa et al.*, 1984; *Lauben et al.*, 2002; *Goldstein and Tsurutani*, 1984]. Values of θ have largely been estimated as less than 30°. Using 18 passes of the OGO5 spacecraft, *Burton and Holzer* [1974] found that θ was less than 30° for $MLat < 40°$ (80% of the events) for the lower band chorus and that θ extended to 85° for $MLat > 40$ with a spreading of the distribution of angles. A similar behavior for upper band chorus waves was determined by *Haque et al.* [2010] on the basis of POLAR measurements, but the direction of propagation was found to be close to the background magnetic field for lower band chorus waves. Here we study the distribution of whistler waves propagation direction for wide range of L-shells and magnetic latitudes. We investigated how the wave amplitudes, the wave-normals, and the field-aligned Poynting flux depends upon the L-shell, the magnetic latitude, and geomagnetic activity (K_p-index) for the region close to the geomagnetic equator ($MLat < 30°$), at radial distances from 2 to 7 R_E as covered by Cluster from 2001 to 2009.

2. Data Set and Analysis Technique

[5] For this work, we utilized a large dataset for VLF waves, as observed by Cluster between January 2001 and August 2009, in an area inside the equatorial radiation belts region (i.e., confined for the ±30° MLat and L-shell ≤ 7). The region is thought to be of primary importance for the generation of chorus waves. The Cluster dataset contains a sufficient number of points for performing a statistical study for the presented range of magnetic local times (MLT) and L-shells, as illustrated in the small panels in Figures 1 and 2a. Our survey included STAFF-SA data from the Cluster 3 spacecraft (Samba) in order to avoid different statistical contributions due to different cross-spacecraft distances during the processing period. Our analysis was primarily based on data from the Spatio-Temporal Analysis of Field Fluctuations - Spectrum Analyzer (STAFF-SA) experiment [*Cornilleau-Wehrlin et al.*, 2003], which provides the complete spectral matrix (the real and the imaginary part) of the three magnetic components as measured by the STAFF search coil magnetometer. The spectral matrix was computed on-board for 27 frequency channels that were logarithmically spaced between 8.8 Hz and 3.56 kHz. The sensitivity of the STAFF search coil magnetometers was $5 \cdot 10^{-3}$ nT Hz$^{-1/2}$ at 1 Hz, and $4 \cdot 10^{-5}$ nT Hz$^{-1/2}$ at 100 Hz and 4 kHz [*Cornilleau-Wehrlin et al.*, 2003]. We excluded measurements with amplitudes

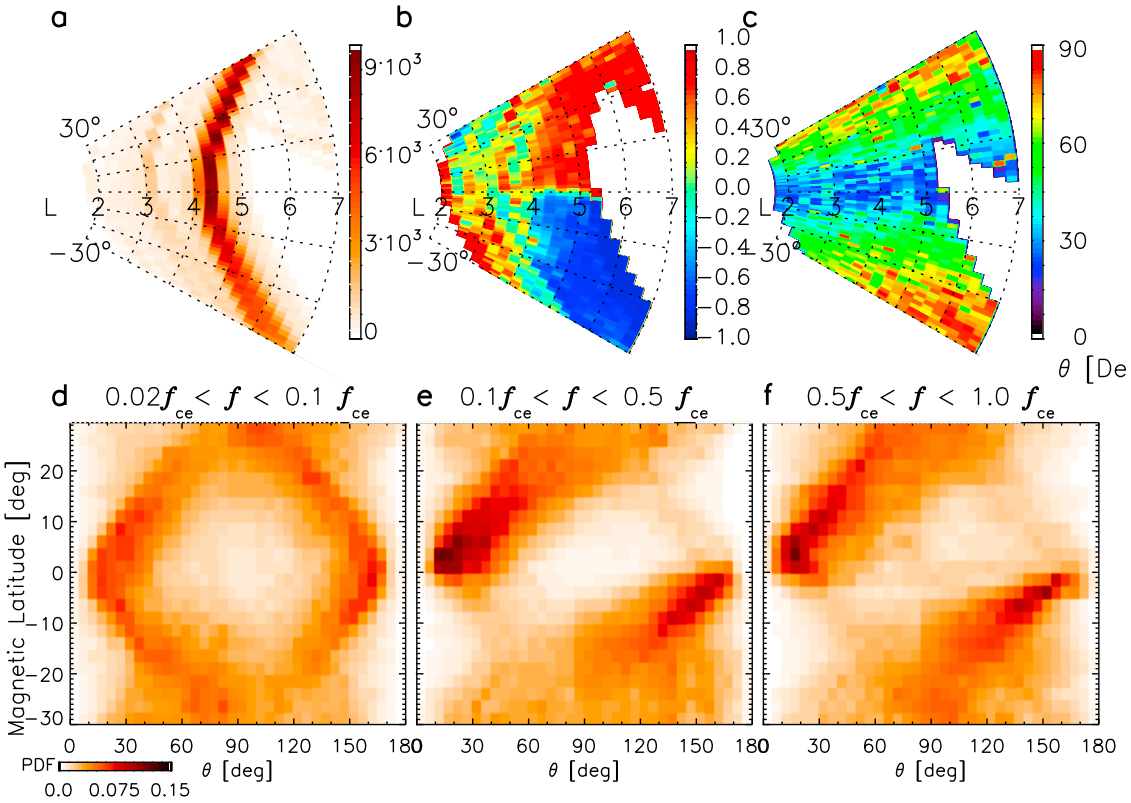

Figure 2. The panels indicate the following: (a) The distribution of CLUSTER STAFF-SA measurements from 2001 to 2009; (b) The dominant direction of the Poynting flux for large amplitude whistler waves in a chorus frequency range ($0.1f_{ce} < f < 1.0f_{ce}$). The direction is characterized by the normalized parameter $(N_a - N_o)/(N_a + N_o)$, where N_a and N_o are the number of spectra having a Poynting flux directed along ($\vec{k} \cdot \vec{B} > 0$) and opposite ($\vec{k} \cdot \vec{B} < 0$) to $\vec{B}$, respectively. The utilized parameter varied from +1 (propagation along $\vec{B}$) to −1 (propagation against $\vec{B}$). (c) The most probable value of the angle between the wave-vector and the local magnetic field direction. The distribution of the angle between the wave-vectors and the background magnetic field for different magnetic latitudes ($4 < L < 7$) (d) for large amplitude hiss waves in the frequency range of ($0.02f_{ce} < f < 0.1f_{ce}$); (e) the large amplitude lower-band chorus frequency range ($0.1f_{ce} < f < 0.5f_{ce}$); and (f) the upper-band chorus wave frequency range ($0.5f_{ce} < f < 1.0f_{ce}$) for L-shell > 5 (STAFF-SA frequency band limitation).

below double the STAFF-SA sensitivity level. The analyzed wave frequency range included electron whistler waves from the lower-hybrid frequency f_{LH} up to the electron cyclotron frequency f_{ce}. The range is known to be dominated by plasmaspheric hiss (from f_{LH} to approximately 0.1 f_{ce}) [*Thorne et al.*, 1973], by the lower-band chorus ($0.1f_{ce} < f < 0.5f_{ce}$), and by the upper-band chorus waves ($0.5f_{ce} < f < 1.0f_{ce}$), but excludes magnetosonic waves which mainly concentrate near the equator (see *Pokhotelov et al.* [2008] for details). Our analysis of magnetosonic waves (not shown) was consistent with the results obtained by *Pokhotelov et al.* [2008] and supplement their results (with observations obtained from 2006 to 2009). Magnetosonic waves are concentrated in the MLT range from 10 to 18, and their normals are mainly perpendicular to B. Hiss waves can be observed above $0.1f_{ce}$ but their intensity rapidly falls above 1 kHz [*Meredith et al.*, 2004], which is close to 0.1 f_{ce} for the main part of STAFF-SA measurements. Local values of f_{ce} were obtained using measurements of FGM flux-gate magnetometers [*Balogh et al.*, 2001]. The value of f_{ce} at the equator was computed using the T96 model [*Tsyganenko*, 1995].

[6] The data analysis was performed using the technique for the wave-normal vector $\vec{k}$ evaluation, as suggested by *Means* [1972], which involves a computation of a spectral matrix that consists of the power and the cross-power spectra using only three magnetic components. The method has an inherent 180° ambiguity in the wave normal direction that can be resolved if the Poynting vector $\vec{S}$ is known, since the wave-normal must have a component in the direction of energy flow and since the scalar product $(\vec{S} \cdot \vec{k})$ should be positive. We calculated the ratio of the eigenvalues [*Goldstein and Tsurutani*, 1984] in order to justify the usage of the single wave approximation (the ratio of the intermediate to smallest eigenvalue needs to be greater than 20). We found that the approximation was not valid only for a very small number of cases, which have a negligible effect on the statistical results. The spectral matrices registered by the STAFF-SA allowed us to evaluate the Poynting flux components along the spacecraft spin axis, and to reconstruct the component along the background magnetic field $\vec{S} = (1/2)Re(\vec{E}(f) \times \vec{B}(f)^*)$. Here, * indicates the complex conjugate, *Re* represents the real part, and $\vec{E}(f)$ and $\vec{B}(f)$ are the Fourier transforms of the electric and the magnetic field waveforms, respectively, the spectral matrix components for 27 frequencies. The third component of the electric field was calculated using the approximation $\vec{B} \cdot \vec{E} = 0$. By applying the procedures described above, we obtained the directions of the wave vectors.

[7] Wave measurements cannot be obtained simultaneously in all of the L-shells, the MLT, and the latitude combinations. Therefore, one may use a statistical approach. Here, the data are presented in the form of probability distribution functions for the wave amplitude and the wave-normal direction. For the statistical study we chose the following parameters: 1) the location of the wave detection (the L-shell, the MLT, and the Magnetic Latitude), 2) the wave characteristics (the wave frequencies normalized to the equatorial values of the electron cyclotron frequency f_{ce}, the magnitude, and the wave-vector direction relative to the background magnetic field), and 3) the geomagnetic activity conditions as characterized by the K_p-index.

3. Statistical Characteristics of VLF Waves in the Inner Magnetosphere

[8] To evaluate the global occurrence rate of whistler waves, the wave magnetic field data was sorted into two categories according to the wave amplitude - low and large amplitude waves. In order to study the statistics of the occurrence of large-amplitude whistler waves, for each of the 27 STAFF-SA frequency channels, we selected events with maximum amplitudes that constituted 20% of the total number of the events in this channel. Figure 1 indicates the occurrence rate of the wave in the chorus (Figure 1, bottom) and the hiss frequency range (Figure 1, top) as the ratio of the number of captured large amplitude waves to the total number of data samples, whose wave amplitudes fell within particular ratios for high amplitude level to total number of samples in each bin. The lower and upper band chorus are shown together because the Cluster STAFF-SA frequency range cannot completely cover the full frequency band of the upper-band chorus [*Pokhotelov et al.*, 2008]. Additionally, it is substantially less intense than the lower-band [*Meredith et al.*, 2001; *Haque et al.*, 2010]. The following three geomagnetic activity regimes are shown: 1) low ($K_p < 3$, left), 2) intermediate ($3 \le K_p \le 5$, middle), and 3) high ($K_p > 5$, right). The chorus and the hiss are distinguished by their frequencies. The range from the equatorial lower hybrid frequency ~$0.02\,f_{ce}$ to $0.1\,f_{ce}$ corresponds to the hiss, and the range from $0.1\,f_{ce}$ to f_{ce} is characteristic of chorus emissions. If the number of spectra in a cell is less than 200 it indicates that the bin was formed by only one trajectory. For this case, the bin is marked as dashed. The summary of all MLT value occurrence rates is shown by a black line. The scale is shown in the right of each panel. The small insets in the bottom-right section of the panels indicate the data coverage (i.e., the total number of captured spectra). The black line plots in each panel show the occurrence rate for large amplitude events as the ratio of the number of captured large amplitude waves to the total number of events in this L-shell bin. The main portion of the intense chorus waves was observed in the MLT range from 6 to 14 MLT, and in the L-shell range from four to seven (Figure 1), for low and intermediate geomagnetic activity ($K_p < 5$). The statistics for high geomagnetic activity are poor, but allowed us to determine that the major portion of large amplitude chorus waves were detected near local noon. In general, the distribution of large amplitude chorus waves becomes more uniform with increasing magnetic activity. The distributions for the chorus and hiss we obtained were similar to those presented by *Pokhotelov et al.* [2008] for averaged wave amplitudes. In this work, we extended their study using Cluster data obtained from 2006 to 2009. Our results are also consistent with previous studies based on measurements aboard the DE-1 [*Andre et al.*, 2002] and additionally provide good statistics for $L = 3 - 7$. The general peculiarities of VLF wave distributions in Figure 1 are also close to those presented by *Meredith et al.* [2001, 2004], *Li et al.* [2009], and *Cully et al.* [2008]. Some of the differences can be explained by different frequency ranges and relatively poor statistics for high geomagnetic activity time intervals.

[9] The prevalent direction of wave propagation along $\vec{B}$ (Poynting flux direction) is shown in Figure 2b. Two regions can be distinguished that show different statistical properties for whistler type emissions, as follows: the region at $L = 2 - 4$, where the hiss and the whistlers generated at high latitudes (lightning generated whistlers) were mainly observed, and the region at $L = 4 - 7$, where chorus type whistlers generated at the equator dominated. The most probable values for the angle between the whistler wave-normal and the local magnetic field are shown in Figure 2c. One can see that the angle increases with magnetic latitude, reaching resonance values at a MLat of ~20°.

[10] The probability distribution function (PDF) of the large amplitude whistler wave-normal direction θ (relative to background $\vec{B}$) on the magnetic latitude for L-shells $4 < L < 7$ is shown in Figures 2d–2f for the hiss, the lower, and the upper band chorus, respectively. The distribution of angles was significantly different from Gaussian. The distribution is nonsymmetric and the width of the distribution increases with latitude. The distribution is formed by two groups of waves. The first group is generated at the equator and propagates toward the poles. The second group is reflected at higher latitudes in the magnetosphere and propagates toward the equator. The spreading of the border, which separates poleward waves above and below the equator, was obtained as a result of the displacement of the magnetic field minimum position from the model magnetic equator in the range of two to five degrees [*Parrot et al.*, 2003]. For both groups, the wave-normals exhibited the same tendency, and their direction deviated stronger from the direction of the magnetic field with an increase in magnetic latitude. The observed asymmetry of the distributions for positive and negative values of geomagnetic latitude appeared due to the non-symmetry of the L-shell covering, above and below the magnetic equator. Whistler waves with small amplitudes do not show such a dependence for wave normal directions, and their distributions are more isotropic for all latitudes. Several important characteristics of our analysis should be taken into account in order to understand the characteristic features of the observed PDFs. Our analysis was performed in the fixed frequency range of the STAFF-SA instrument (8.8 Hz – 3.56 kHz). Waves at higher latitudes (stronger B) have a smaller range of ratios (f/f_{ce}), which results in a larger deviation in the wave-normals from the direction of the magnetic field. On the other hand, waves detected at a particular location at higher magnetic latitudes are generated at different L-shells at the equator, resulting in a larger angular width of the distribution. At higher latitudes the background magnetic field increases along the wave ray-path, the wave frequencies become closer to the local lower-hybrid frequency, the wave-normals deviate toward the perpendicular direction, and, finally, the wave-normals become perpendicular to $\vec{B}$ for wave frequencies below the local lower-

hybrid frequency. As the wave-normal becomes more oblique, the component of the wave-vector along $\vec{B}$ becomes smaller, and both the parallel and the perpendicular components of the group velocity decrease. Therefore, waves propagate slower at higher latitudes, and spend more time in high-altitude regions, giving rise to a peak in the statistical amplitude distribution at ~90°. The same effect results in similar properties for the distributions of the reflected waves propagating toward the equator (group 2). At higher latitudes, both poleward (group 1) and equatorward (group 2) propagating waves shift toward perpendicular angles and the energy flux of the reflected waves becomes relatively larger. The two peaks of the distribution approach one another and the frequency becomes close to the lower-hybrid frequency. At magnetic latitudes of approximately 30° the two peaks merge, forming a common distribution with a peak spread of approximately 90° and having an angular width of the same order.

4. Conclusions

[11] In this work, we present the probability distribution of wave amplitudes and wave-normals based on a statistical study of wave measurements obtained from the Cluster satellite from 2001 to 2009. The statistical database spans the equatorial radiation belts region, L-shells from two to seven, at various magnetic latitudes for quiet, moderate, and active geomagnetic conditions. The analysis was performed in the frequency range from 8.8 Hz to 3.56 kHz by making use of STAFF-SA measurements. The most intense chorus waves were observed in the range from 6 to 14 hours MLT and for L-shells from four to seven; and for hiss waves, from 11 to 19 hours MLT and for L-shells from 2.5 to 3.5, (this maximum was shown by *Andre et al.* [2002] for the DE-1 dataset). The statistical characteristics of the distributions were different for low, moderate ($K_p < 5$), and high ($K_p > 5$) geomagnetic activity. Two distinguishable regions exist for which the statistical properties of the wave amplitudes and the wave-normal distributions exhibited different statistical characteristics under low and moderate geomagnetic activity, as follows: 1) from $L = 2 - 4$ (to the plasmapause) where lightning generated and magnetospheric hiss whistlers dominated; and 2) in a region where chorus-type whistlers dominated, from $L = 4 - 7$. The obtained distributions of the chorus and hiss wave amplitudes extended to the database as presented by *Pokhotelov et al.* [2008], with Cluster data for 2006 to 2009. Our study also extended the VLF wave statistics for L-shells three to seven for the existing databases based on DE-1, CRRES, and THEMIS measurements. In general, our results are consistent with the earlier obtained results of *Li et al.* [2009], *Meredith et al.* [2001, 2004], *Andre et al.* [2002], *Green et al.* [2005], *Cully et al.* [2008], and *Pokhotelov et al.* [2008].

[12] For the first time, we have obtained a statistical distribution for wave-normal directions as a function of magnetic latitude. The distribution of θ (the angle between the wave-vector and the background magnetic field) at the geomagnetic equator was concentrated in a 30° cone, with a maximum around 20°. Our results are similar to results based on measurements in the vicinity of the geomagnetic equator as presented by *Burton and Holzer* [1974], *Hayakawa et al.* [1984], and *Agapitov et al.* [2010]. With increasing magnetic latitude, the distribution drifts toward more oblique to the background magnetic field wave-normals, reaching resonance angles of ~15° − 20°, consistent with results obtained for chorus waves by *Burton and Holzer* [1974] and *Muto et al.* [1987] for the lower band chorus, by *Haque et al.* [2010] for the upper band chorus, and by *Hayakawa et al.* [1986] for hiss. Wave-vector behavior is consistent with the statement by *Lauben et al.* [2002] that upper band choruses are generated near the equator with a wave-vector approximately along the background magnetic field, and that their propagation away from the equator quickly moves the wave-vector angles close to the resonance cone. The similar tendency for the lower band chorus indicated that their generation in the vicinity of the equator, with wave-vectors directed close to the background magnetic field but not along to it, is also allowed. The probability distribution of wave activity parameters is usually non-symmetric and has significant non-Gaussian tails. Therefore, one can suggest that they cannot be well-described by averaged amplitude values.

[13] Our results have important implications for descriptions of the of the diffusion processes due to wave-particle interactions. The STAFF-SA data provided the possibility for a statistical study of the distribution of wave-vector directions. The obtained results for VLF wave polarization properties (particularly the drift of the angular wave normal distribution along its ray path) can sufficiently impact conditions of resonance for wave particle interactions, limiting the region where it could be efficient. Conventional averaging procedures could not be performed without taking into account the relatively rapid departure of wave normal vectors from the quasi-parallel propagation conditions. Therefore, they should take into account more realistic wave energy and wave-normal distributions.

[14] **Acknowledgments.** This work was supported by CNES through the grant "Modeles d'ondes", and by the ECO NET program of the EGIDE (France). The research of YK is supported by the Swedish Research Council, grant 2007-4377. We thank the ESA Cluster Active Archive for providing the STAFF-SA dataset.

[15] The Editor thanks two anonymous reviewers for their assistance in evaluating this paper.

References

Agapitov, O., et al. (2010), Chorus source region localization in the Earth's outer magnetosphere using THEMIS measurements, *Ann. Geophys.*, *28*, 1377–1386.

Albert, J. M., N. P. Meredith, and R. B. Horne (2009), Three-dimensional diffusion simulation of outer radiation belt electrons during the 9 October 1990 magnetic storm, *J. Geophys. Res.*, *114*, A09214, doi:10.1029/2009JA014336.

Andre, R., F. Lefeuvre, F. Simonet, and U. S. Inan (2002), A first approach to model the low-frequency wave activity in the plasmasphere, *Ann. Geophys.*, *20*, 981—996.

Balogh, A., et al. (2001), The Cluster magnetic field investigation: Overview of in-flight performance and initial results, *Ann. Geophys.*, *19*, 1207–1217.

Bourdarie, S., D. Boscher, T. Beutier, J.-A. Sauvaud, and M. Blanc (1996), Magnetic storm modeling in the Earth's electron belt by the Salammbô code, *J. Geophys. Res.*, *101*, 27,171–27,176.

Burton, R. K., and R. E. Holzer (1974), The origin and propagation of chorus in the outer magnetosphere, *J. Geophys. Res.*, *79*, 1014–1023.

Cornilleau-Wehrlin, N., et al. (2003), First results obtained by the Cluster STAFF experiment, *Ann. Geophys.*, *21*, 437–456.

Cully, C. M., J. W. Bonnell, and R. E. Ergun (2008), THEMIS observations of long-lived regions of large-amplitude whistler waves in the inner magnetosphere, *Geophys. Res. Lett.*, *35*, L17S16, doi:10.1029/2008GL033643.

Fok, M.-C., R. B. Horne, N. P. Meredith, and S. A. Glauert (2008), Radiation Belt Environment model: Application to space weather nowcasting, *J. Geophys. Res.*, *113*, A03S08, doi:10.1029/2007JA012558.

Glauert, S. A., and R. B. Horne (2005), Calculation of pitch angle and energy diffusion coefficients with the PADIE code, *J. Geophys. Res.*, *110*, A04206, doi:10.1029/2004JA010851.

Goldstein, B. E., and B. T. Tsurutani (1984), Wave normal directions of chorus near the equatorial source region, *J. Geophys. Res.*, *89*, 2789–2810.

Green, J. L., S. Boardsen, L. Garcia, W. W. L. Taylor, S. F. Fung, and B. W. Reinisch (2005), On the origin of whistler mode radiation in the plasmasphere, *J. Geophys. Res.*, *110*, A03201, doi:10.1029/2004JA010495.

Haque, N., M. Spasojevic, O. Santolík, and U. S. Inan (2010), Wave normal angles of magnetospheric chorus emissions observed on the Polar spacecraft, *J. Geophys. Res.*, *115*, A00F07, doi:10.1029/2009JA014717.

Hayakawa, M., Y. Yamanaka, M. Parrot, and F. Lefeuvre (1984), The wave normals of magnetospheric chorus emissions observed on board GEOS 2, *J. Geophys. Res.*, *89*, 2811–2821.

Hayakawa, M., N. Ohmi, M. Parrot, and F. Lefeuvre (1986), Direction finding of ELF hiss emissions in a detached plasma region of the magnetosphere, *J. Geophys. Res.*, *91*, 135–141.

Lauben, D. S., U. S. Inan, T. F. Bell, and D. A. Gurnett (2002), Source characteristics of ELF/VLF chorus, *J. Geophys. Res.*, *107*(A12), 1429, doi:10.1029/2000JA003019.

Li, W., R. M. Thorne, V. Angelopoulos, J. Bortnik, C. M. Cully, B. Ni, O. LeContel, A. Roux, U. Auster, and W. Magnes (2009), Global distribution of whistler-mode chorus waves observed on the THEMIS spacecraft, *Geophys. Res. Lett.*, *36*, L09104, doi:10.1029/2009GL037595.

Lyons, L. R. (1974a), General relations for resonant particle diffusion in pitch angle and energy, *J. Plasma Phys.*, *12*, 45–49.

Lyons, L. R. (1974b), Pitch angle and energy diffusion coefficients from resonant interactions with ion-cyclotron and whistler waves, *J. Plasma Phys.*, *12*, 417–432.

Lyons, L. R., and R. M. Thorne (1973), Equilibrium structure of radiation belt electrons, *J. Geophys. Res.*, *78*, 2142–2149, doi:10.1029/JA078i013p02142.

Means, J. D. (1972), Use of the three-dimensional covariance matrix in analyzing the polarization properties of plane waves, *J. Geophys. Res.*, *77*, 5551–5559.

Meredith, N. P., R. B. Horne, and R. R. Anderson (2001), Substorm dependence of chorus amplitudes: Implications for the acceleration of electrons to relativistic energies, *J. Geophys. Res.*, *106*, 13,165–13,178.

Meredith, N. P., R. B. Horne, R. M. Thorne, D. Summers, and R. R. Anderson (2004), Substorm dependence of plasmaspheric hiss, *J. Geophys. Res.*, *109*, A06209, doi:10.1029/2004JA010387.

Muto, H., M. Hayakawa, M. Parrot, and F. Lefeuvre (1987), Direction finding of half-gyrofrequency VLF emissions in the off-equatorial region of the magnetosphere and their generation and propagation, *J. Geophys. Res.*, *92*, 7538–7550.

Omura, Y., D. Nunn, H. Matsumoto, and M. J. Rycroft (1991), A review of observational, theoretical and numerical studies of VLF triggered emissions, *J. Atmos. Terr. Phys.*, *53*, 351—368.

Parrot, M., O. Santolik, N. Cornilleau-Wehrlin, M. Maksimovic, and C. C. Harvey (2003), Source location of chorus emissions observed by Cluster, *Ann. Geophys.*, *21*, 473–480.

Pokhotelov, D., F. Lefeuvre, R. B. Horne, and N. Cornilleau-Wehrlin (2008), Survey of ELF-VLF plasma waves in outer radiation belt observed by Cluster STAFF-SA experiment, *Ann. Geophys.*, *26*, 3269–3277.

Sazhin, S. S., and M. Hayakawa (1992), Magnetospheric chorus emissions: A review, *Planet. Space Sci.*, *40*, 681–697.

Shprits, Y. Y., D. A. Subbotin, N. P. Meredith, and S. R. Elkington (2008), Review of modeling of losses and sources of relativistic electrons in the outer radiation belt II: Local acceleration and loss, *J. Atmos. Sol. Terr. Phys.*, *70*, 1694—1713.

Thorne, R., E. Smith, R. Burton, and R. Holzer (1973), Plasmaspheric hiss, *J. Geophys. Res.*, *78*, 1581–1596.

Tsyganenko, N. A. (1995), Modeling the Earth's magnetospheric magnetic field confined within a realistic magnetopause, *J. Geophys. Res.*, *100*, 5599–5612.

O. Agapitov, Astronomy and Space Physics Department, National Taras Shevchenko University of Kiev, Academic Glushkov Avenue, 2, 03121 Kiev, Ukraine. (agapit@univ.kiev.ua)

Y. V. Khotyaintsev, Swedish Institute of Space Physics, Box 537, SE-751 21 Uppsala, Sweden.

V. Krasnoselskikh, LPC2E, CNRS, 3A, Avenue de la Recherche Scientifique, F-45071 Orleans CEDEX, France.

G. Rolland, CNES, 18 Avenue Edouard Belin, F-31401 Toulouse CEDEX 4, France.